The Anthelmintic Drug Mebendazole Induces Mitotic Arrest and Apoptosis by Depolymerizing Tubulin in Non-Small Cell Lung Cancer Cells[1]

Ji-ichiro Sasaki, Rajagopal Ramesh, Sunil Chada, Yoshihito Gomyo, Jack A. Roth, and Tapas Mukhopadhyay[2]

Section of Thoracic Molecular Oncology, Departments of Thoracic and Cardiovascular Surgery [J. S., R. R., Y. G., J. A. R., T. M.] and Molecular and Cellular Oncology [J. A. R.], The University of Texas M. D. Anderson Cancer Center, and Introgen Therapeutics Inc. [S. C.], Houston, Texas 77030

Abstract

Microtubules have a critical role in cell division, and consequently various microtubule inhibitors have been developed as anticancer drugs. In this study, we assess mebendazole (MZ), a microtubule-disrupting anthelmintic that exhibits a potent antitumor property both *in vitro* and *in vivo*. Treatment of lung cancer cell lines with MZ caused mitotic arrest, followed by apoptotic cell death with the feature of caspase activation and cytochrome *c* release. MZ induces abnormal spindle formation in mitotic cancer cells and enhances the depolymerization of tubulin, but the efficacy of depolymerization by MZ is lower than that by nocodazole. Oral administration of MZ in mice elicited a strong antitumor effect in a s.c. model and reduced lung colonies in experimentally induced lung metastasis without any toxicity when compared with paclitaxel-treated mice. We speculate that tumor cells may be defective in one mitotic checkpoint function and sensitive to the spindle inhibitor MZ. Abnormal spindle formation may be the key factor determining whether a cell undergoes apoptosis, whereas strong microtubule inhibitors elicit toxicity even in normal cells.

Introduction

Lung cancer has become the leading cause of cancer death in the world (1). NSCLC,[3] the most common type of lung cancer, has a poor prognosis despite improvements in early diagnosis and treatment. More than 75% of patients with NSCLC become candidates for chemotherapy at some point during the course of their disease because of the development of systemic metastases (2). However, chemotherapy for NSCLC still produces poor response rates, with a relatively short duration of response and rare complete remissions. Exploring molecular targets of sensitivity or resistance to chemotherapy for NSCLC, as well as for other solid tumors, may help improve the efficacy of various chemotherapy regimens. Although the primary intracellular molecular targets of anticancer drugs vary, tubulin, the major protein component of microtubules, is one such target (3). In fact, microtubule-stabilizing agents such as paclitaxel and docetaxel or microtubule-disrupting agents such as vinorelbine are active against NSCLC (4–6). Disrupting the dynamics of tubulin polymerization or depolymerization and the functions of microtubules with these drugs induces mitotic arrest and apoptosis in dividing cancer cells (7).

MZ (methyl 5-benzoyl-2-benzimidazole-carbamate) is a broad-spectrum anthelmintic drug that has been used to treat helminthic diseases in humans all over the world. Benzimidazole carbamates have been reported to inhibit the polymerization of tubulins and to disrupt the function of microtubules in parasite cells (8, 9). Results from drug binding studies using enriched extracts of helminthic and mammalian tubulin have suggested that tubulin is the primary molecular target of the benzimidazoles (10). Clinically, two benzimidazole derivatives, MZ and albendazole [methyl (5-propylthio)-1*H*-benzimidazol-2-yl carbamate methylester] have been used to treat human alveolar echinococcosis, a lethal pulmonary helminthic infection. The metacestode stage of *Echinococcus multilocularis*, the causative agent of this disease, has characteristics of a malignant tumor, including invasive growth and metastasis formation (11). Although echinococcosis requires long-term treatment with MZ, the incidence of severe side effects to the host has been quite low (12, 13). Because the drug acts by inhibiting microtubule formation and because its delivery to human peripheral lung tissue has few or no side effects, we assumed that MZ may have an antitumor effect on human lung cancer. However, during the course of our study, reports have been published regarding the use of anthelmintic benzimidazoles in human cancer. Pourgholami *et al.* (14) reported that albendazole induced growth inhibition of human hepatocellular carcinoma cells both *in vitro* and *in vivo*. These results led to a subsequent pilot study of albendazole in patients with advanced hepatocellular carcinoma or with colorectal cancer with liver metastases (15).

In this study, we show that MZ is a mild spindle inhibitor but possesses a potent antitumor effect, as evident from *in*

[3] The abbreviations used are: NSCLC, non-small cell lung cancer; z-VAD, Z-Val-Ala-Asp (OMe)-CH$_2$F; FMK, Z-Val-Ala-Acp-(OMe)-CH$_2$F; MZ, mebendazole; XTT, 2,3-bis[2-methoxy-4-nitro-5-sulfophenyl]-2*H*-tetrazolium-5-carboxanilide inner salt; PI, propidium iodide; TUNEL, terminal deoxynucleotidyl transferase-mediated nick end labeling; PARP, poly(ADP-ribose) polymerase.

vitro and *in vivo* studies. *In vivo*, the effect on s.c. NSCLC xenografts and in lung metastasis studies indicated that MZ inhibits tumor cell growth by inducing apoptosis in tumor cells and spare normal cells.

Materials and Methods

Chemicals. MZ (Sigma-Aldrich, St. Louis, MO) was dissolved in DMSO to a concentration of 10 mM and stored at –20°C as a master stock solution. Paclitaxel was purchased from Bristol-Myers Squibb Company (Princeton, NJ), and nocodazole was purchased from Sigma-Aldrich.

Cell Growth Assay. H460, A549, H1299, and WI-38 cell lines were obtained from the American Type Culture Collection (Manassas, VA) and maintained according to the supplier's instructions. Cells were seeded at a density of 1×10^4 cells/well on either RPMI 1640 or F12 medium supplemented with 10% heat-inactivated FCS and antibiotics in 24-well culture plates and then treated with MZ or with 0.1% DMSO as a control. Cells then were trypsinized and counted by the trypan blue method every day for 4 days. All experiments were done in triplicate.

Cell Survival Assay. Forty-eight h after drug treatment, cytotoxicity was assessed by the XTT assay (Roche Diagnostics, Mannheim, Germany) in 96-well microtiter culture plates as per the manufacturer's instructions. UV absorbance values were normalized to the values obtained for the untreated cells to determine the percentage of surviving cells. The IC_{20}, IC_{50}, and IC_{80} values were the drug concentrations that induced 20%, 50%, and 80% reductions in absorbance according to the Curve Fit 1.3 program. The difference between the percentages of surviving cells in the untreated cells and the z-VAD-FMK-treated cells was tested for statistical significance by Student's *t* test. The significance level was set at $P < 0.05$.

Apoptosis and Flow Cytometric Analysis of Cell Cycle. Apoptotic cells with characteristic nucleosomal DNA degradation were examined in control untreated cells and after 24 and 48 h of MZ treatment, as described previously (16). Cells were treated with either DMSO or MZ for 24 or 48 h, both floating and attached cells were harvested, and cell pellets were lysed in 100 μl of lysis buffer [10 mM Tris (pH 7.4), 10 mM EDTA (pH 8.0), and 0.5% Triton X-100] and incubated for 10 min at 4°C. DNA released in the supernatants was incubated with 200 μg/ml RNase A for 1 h at 37°C and then with 200 μg/ml proteinase K for 30 min at 50°C. DNA was extracted and precipitated with 0.5 M NaCl and 50% isopropanol. The samples were loaded onto 2% agarose gels and stained with ethidium bromide.

After appropriate treatments, cells were harvested, washed in PBS, and fixed in 70% methanol. The fixed cells were incubated with 0.65 μg/ml mouse monoclonal anti-MPM-2 antibody as described previously (17). Cells were then incubated with 2 μg/ml FITC-conjugated goat anti-mouse IgG secondary antibody (Santa Cruz Biotechnology, Santa Cruz, CA), 20 μg/ml PI (Roche Diagnostics), and 10 μg/ml RNase A (Sigma-Aldrich) at 37°C for 30 min and processed for cell cycle analysis using an EPICS Profile II flow cytometer (Coulter Corp., Miami, FL) with the Multicycle

Phoenix Flow Systems program (San Diego, California). All experiments were repeated at least twice.

Cytosolic and Mitochondrial Fractionation of Cytochrome *c* and Western Blotting. We examined the level of cytochrome *c* in the cytosolic extracts of control and MZ-treated cells using an ApoAlert Cell Fractionation Kit (Clontech, Palo Alto, CA) according to the manufacturer's user's manual. The protein concentrations were determined by using the Bradford method (Bio-Rad, Hercules, CA). Then, 25 μg of the protein were used for immunoblotting as described previously (18). These experiments were repeated at least three times. To prepare whole-cell lysates, cells were lysed in 1× SDS sample buffer [62.5 mM Tris-HCl (pH 6.8), 2% SDS, 10% glycerol, 1× proteinase inhibitor mixture (Complete; Roche), and 6 M urea]. Then, 50 μg of the protein were used for immunoblotting as described previously (18). Rabbit polyclonal anti-AIK (human Aurora A kinase) antibodies were kindly given by Drs. Tomotoshi Marumoto and Hideyuki Saya (Kumamoto University School of Medicine, Kumamoto, Japan). Mouse monoclonal and rabbit polyclonal antibodies used as primary antibodies included anti-cyclin A (CY-A1; Sigma-Aldrich), anti-cyclin B1 (GNS1; Lab Vision Corp., Fremont, CA), anti-cyclin E (HE-12; BD Biosciences, San Diego, CA), anti-cdc2 p34 (17; Santa Cruz Biotechnology), anti-cdc25C (C-20; Santa Cruz Biotechnology), anti-p53 (Bp53-12; Santa Cruz Biotechnology), anti-p21 (Ab-1; Oncogene Research Science, Cambridge, MA), anti-p27 (Bp53-12; Santa Cruz Biotechnology), anti-bcl-2 (100; Santa Cruz Biotechnology), anti-bcl-xl (H-5; Santa Cruz Biotechnology), anti-β-actin (AC-15; Sigma-Aldrich), anti-PARP (4C10–5; BD Biosciences), anti-caspase 3 (catalogue number 556425; BD Biosciences), anti-caspase 8 (H-134; Santa Cruz Biotechnology), and anti-caspase 9 (catalogue number 9502; Cell Signaling Technology, Beverly, MA).

Immunofluorescence Microscopy. Cells were grown on a glass chamber slide and treated with 0.1% DMSO, 0.5 μM MZ, 50 nM nocodazole, or 10 nM paclitaxel for 14 h. Cells were then washed with PBS and permeabilized with microtubule-stabilizing buffer [80 mM PIPES-KOH (pH 6.8), 5 mM EGTA, and 1 mM MgCl₂ containing 0.5% Triton X-100] for 5 min at room temperature before being fixed with chilled absolute methanol for 10 min at –20°C as described elsewhere (19). After being washed, cells were incubated with monoclonal mouse anti-α-tubulin antibody (Sigma) for 1 h at room temperature. This was followed by incubation with FITC-conjugated antimouse IgG antibody (Santa Cruz Biotechnology). The stained cells were mounted with Vectashield (Vector Laboratories, Burlingame, CA) and observed by fluorescence microscopy.

Measurement of Soluble and Assembled Tubulin. Soluble (depolymerized) tubulin and assembled (polymerized) tubulin were measured as described previously with some modifications (20, 21). Briefly, cells were treated with DMSO, MZ, vinorelbine, or paclitaxel for 4 h. Cells were then washed with PBS, lysed with 100 μl of lysis buffer [20 mM Tris-HCl (pH 6.8), 0.5% NP40, 1 mM MgCl₂, 2 mM EGTA, and 0.5 μg/ml paclitaxel], mixed with a vortex mixer, and centrifuged at 12,000 × *g* for 10 min at 4°C. Supernatants containing soluble tubulin were separated

from pellets containing polymerized tubulin and placed in separate tubes. The pellets were resuspended in 100 μl of water. The cytosolic and cytoskeletal fractions were dissolved in lysis buffer and separated by SDS-PAGE. Immunoblots were probed with both monoclonal mouse anti-α-tubulin and anti-β-actin antibody (Sigma). The band of each sample was quantified by using the NIH Image program, and the ratios of depolymerized *versus* polymerized tubulin were calculated for each treatment condition. The ratios of depolymerized *versus* polymerized actin were also determined as an internal control. The *t* test was used to analyze significant differences between the ratios of depolymerization/polymerization of tubulin and actin in control cells and those in treated cells. Significance was assumed at the level of $P < 0.05$.

Effect of MZ on s.c. Tumor Growth in Nude Mice. The antitumor effect of MZ on H460 xenografts was examined by s.c. inoculation of 10^6 cells in irradiated (3.5 Gy) *nude* mice (Charles River, Wilmington, MA). When tumors reached ~5 mm in diameter, the animals were randomly assigned to receive either water or oral MZ (1 mg/mouse) every other day for 3 weeks. MZ was given as chewable tablets (Vermox; Janssen Pharmaceutica, Titusville, NJ) that had been homogenized and resuspended in water for oral administration. Tumor diameters were measured every 7 days, and tumor volumes were calculated with the formula $a^2 \times b/2$ (in which *a* is the short diameter of the tumor, and *b* is the long diameter of the tumor). Five animals were used in each group, and each experiment was repeated twice. Differences in tumor volumes between the control and MZ-treated mice at the indicated time points were analyzed with *t* tests, with the level of statistical significance set at $P < 0.05$.

TUNEL Staining. After treatment with H_2O or MZ, H460 s.c. tumors were harvested to make frozen tissue samples. Using these samples, TUNEL staining was performed according to the user's manual of the *In Situ* Cell Death Detection Kit (Roche). In brief, frozen section (6 μm) were fixed in 4% paraformaldehyde for 20 min. After a wash in PBS, the tissue sections were incubated in permeabilization buffer (0.1% Triton X-100 and 0.1% sodium citrate) for 1 min on ice. After two rinses with PBS, samples were incubated in 50 μl of TU NEL reaction mixture for 60 min. We detected labeled ends as fluorescent signals (green) under fluorescence microscopy.

Effect of MZ and Paclitaxel on Experimental Lung Metastasis. A549 cells (2 $\times$ 10^6 cells/animal) were injected through the tail vein of *nude* mice (Charles River) that had received 3.5 Gy of total body irradiation 1 day before injection. Mice were then given MZ suspension (1 mg/mouse every other day) or paclitaxel (1 mg/mouse, 3 days) starting 5 days after cell injection. To serve as untreated controls, another group of mice was given the same volume of PBS. Animals were killed 21 days after injection. Their lungs were harvested and fixed with Fekete's solution (60% ethanol, 3% formaldehyde, and 4% glacial acetic acid) after intratracheal injection of a 15% India ink solution. The total number of unstained colonies on the lung surface was counted under a stereoscopic microscope.

Results

MZ Inhibits the Growth of Human NSCLC Cell Lines *in Vitro*. Treatment of the H460 and A549 human NSCLC cell lines with MZ at doses as low as 0.1 μM significantly suppressed cell proliferation relative to that of cells treated with DMSO (Fig. 1*A*). At the dose range tested (0.1–10 μM), MZ reduced cell survival (as determined by XTT assay) by no more than 40% for normal lung fibroblasts, although it inhibited NSCLC cell viability by more than 50% at doses of 0.2–0.5 μM (Fig. 1*B*). The IC$_{50}$ values for MZ for A549, H1299, and H460 cell lines tested are 0.417 $\pm$ 0.038, 0.26 $\pm$ 0.008, and 0.203 $\pm$ 0.012 μM, respectively. The IC$_{80}$ value for H460 cells is 0.523 $\pm$ 0.021 μM; therefore, we set 0.5 μM as a standard dose for *in vitro* experiments. The IC$_{80}$ could not be obtained for H1299 and A549 cells because the maximum MZ dose used (10 μM) produced only about 75% suppression in those cell lines. Of the NSCLC cell lines analyzed, H460 cells were the most sensitive to MZ, and A549 cells were the most resistant to MZ. Because both cell lines have a wild-type p53 gene, sensitivity to MZ is not associated with the *p53 genotype*.

Induction of Mitotic Arrest after MZ Treatment. Flow cytometric analysis of H460 cell cycle profiles after MZ treatment showed that a 0.5-μM dose led to an accumulation of cells with 4N DNA contents and a concomitant decrease in cells with 2N DNA until 12 h after treatment (Fig. 1*C*, *top panels*). At that time, the cells were round, and most had evidence of nuclear condensation and disruption of nuclear membranes on Hoechst nuclear staining (data not shown). These observations provided the indirect evidence that MZ induced mitotic arrest in cancer cells. To confirm and quantify the incidence of mitotic arrest, we performed two-dimensional flow cytometric analysis of H460 cells stained with either PI or anti-MPM-2 antibodies after MZ treatment. The proportions of mitotic and 4N cells increased over time after MZ treatment (Fig. 1*C*, *bottom panels,* and *D*). Levels of proteins known to regulate the cell cycle were also affected by MZ treatment in both H460 and A549 cells. Amounts of cyclins A and E were reduced at 6–12 h after MZ treatment, but levels of cyclin B1 and AIK, an M-phase kinase, reached a peak at 12 h (Fig. 2*A*). Moreover, shifts in the types of the cell cycle proteins were also observed. The presence of slower-migrating forms of the Cdc25C phosphatase were observed in both cell lines, and Bcl-2 was observed in H460 cells at 6 h after MZ treatment (Fig. 2*A*). The relative expression of Bcl-2 and Bcl-xl differed in the two NSCLC cell lines, with Bcl-2 predominant in H460 cells and Bcl-xl predominant in A549 cells, as reported previously (22). Similar changes in protein expression or modification were observed in both cell lines after treatments with other microtubule-damaging agents such as paclitaxel or vinorelbine (data not shown). Although no change in the expression level of the cyclin-dependent kinase inhibitor protein p27 was detected after MZ treatment of either cell line, p21 protein was up-regulated after 24 h, with accumulation of p53 (Fig. 2*A*). The elevation of p21 and p53 proteins was observed at the same time as the increase in the proportion of cells in sub-G$_0$/G$_1$ and G$_1$ (Figs. 1*C* and 2, *A* and *B*).
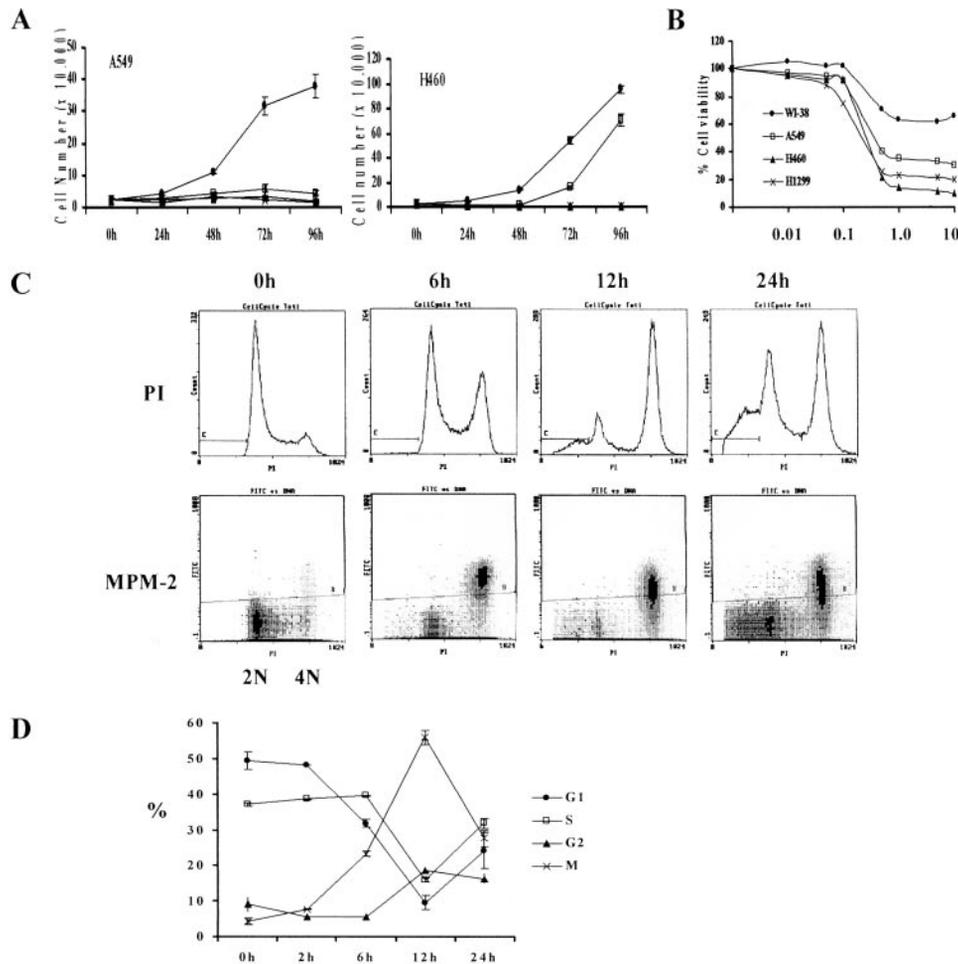
Fig. 1.   Mebendazole suppresses growth and induces mitotic arrest in NSCLC cells. *A,* cell proliferation assays of A549 and H460 cells. Cells were treated with DMSO (●) or with 0.1 (□), 0.5 (▲) or 1 μM (X) mebendazole for 96 h sequentially. As indicated by cell counts, MZ significantly suppressed cell growth after 48 h of incubation, even at the lowest concentration used. *B,* dose-response curves of MZ by XTT assay 48 h after treatment in normal fibroblasts (WI-38) and three NSCLC cell lines (A549, H460, and H1299). Each *curve* is representative of more than three independent experiments. *C,* flow cytometric analysis was performed in asynchronized H460 cells after treatment with 0.5 μM MZ for the indicated time. The cells were trypsinized, fixed, and stained with antibodies to the mitotic epitope MPM-2 and with PI. Histograms (*top panels*) show the proportion of DNA contents in H460 cells after MZ treatment. MZ led to an accumulation of cells with 4N DNA contents and a concomitant decrease in cells with 2N DNA until 12 h after treatment. Scatter graphs (*bottom panels*) reveal that the proportions of mitotic and 4N cells increased over time after MZ treatment. The *lines* in the *top panels* represent the sub-G_0/G_1 fraction, and the *lines* in *bottom panels* indicate the cutoff line of MPM-2-positive cells. *D,* percentages of cells in the G_1, S, G_2, and M phases were calculated and plotted after the indicated time course of MZ treatment in H460 cells. Values are means ± SD from two independent experiments.

***In Vitro* Induction of Apoptosis after MZ Treatment.** MZ significantly increased the proportion of subdiploid cells at 24 h after treatment in both H460 and A549 cell lines (Figs. 1*D* and 2*B*). At 48 h, 35% of H460 cells and 15% of A549 cells were in sub-G_0/G_1 (Fig. 2*B*), indicating that MZ induced cell death after mitotic arrest. To confirm that the cell death was caused by apoptosis, we performed a DNA ladder assay with different MZ doses and found that ladders appeared in a dose-dependent manner in both cell lines 48 h after MZ treatment (Fig. 2*C*). In both cell lines, MZ dramatically released cytochrome *c* from mitochondria to cytosol in a dose-dependent manner 24 h after treatment (Fig. 2*D*) but not at 6 or 12 h after treatment (data not shown). This time course was consistent with that of the increase in the proportion of subdiploid cells. With regard to caspase activation, we detected caspase 3, caspase 9, caspase 8, and PARP cleavage in a dose-

dependent manner 48 h after MZ treatment (Fig. 2*E*). Levels of the apoptotic Bcl-2 family proteins such as Bax, Bak, and Bid did not change (data not shown). The use of ELISA confirmed that MZ treatment activated caspase 3, as compared with no treatment or DMSO treatment of H460 cells (data not shown). Moreover, z-VAD-FMK, a broad-spectrum caspase inhibitor, improved H460 cell survival after MZ treatment, but this effect did not exceed 15% even at the maximum z-VAD-FMK concentration (Fig. 2*F*).

MZ Inhibits Normal Spindle Formation. MZ had no effect on microtubule formation in A549 cells at interphase (Figs. 3*C*). Normal spindle formation was also confirmed in dividing cells that had been treated with DMSO (Fig. 3*B*). At 14 h after MZ treatment, many mitotic cells had abnormally reduced numbers of spindles or had monopolar (monoaster) spindles (Fig. 3*D*). These spindle abnormalities were very

Fig. 2. MZ induces apoptosis in NSCLC cells. *A,* MZ induced changes in the expression and phosphorylation status of proteins known to regulate the cell cycle or apoptosis in both A549 and H460 cells. Asynchronized cells were treated with 0.5 μM MZ for the indicated time. Proteins were extracted from the cells for immunoblot analysis. *Arrows* represent phosphorylated forms of Cdc25C and Bcl-2 protein. Anti-β-actin monoclonal antibody was used as the loading control. *B,* the percentage of subdiploid cells (cells in sub-G_0/G_1) was measured after MZ treatment for the indicated time in H460 and A549 cells. Values are means $\pm$ SD from three independent experiments. *C,* nucleosomal DNA degradation was analyzed in H460 and A549 cells at 48 h after MZ treatment with the indicated doses. DNA fragmentation was detected by 2% agarose gel electrophoresis in a dose-dependent manner in both cell lines. *D,* release of cytochrome *c* (*Cyto C*) from mitochondria to cytosol was detected in both A549 and H460 cells 24 h after MZ treatment by immunoblotting. *E,* cleavages of caspases (*Cas*) and PARP were detected 48 h after MZ treatment. *Arrows* represent the cleaved proteins. *F,* z-VAD-FMK enhanced cell survival after treatment with 0.5 μM MZ in H460 cells. Values are means $\pm$ SD from three independent experiments. The significance level was set at $P < 0.05$. ∗, $P < 0.05$.
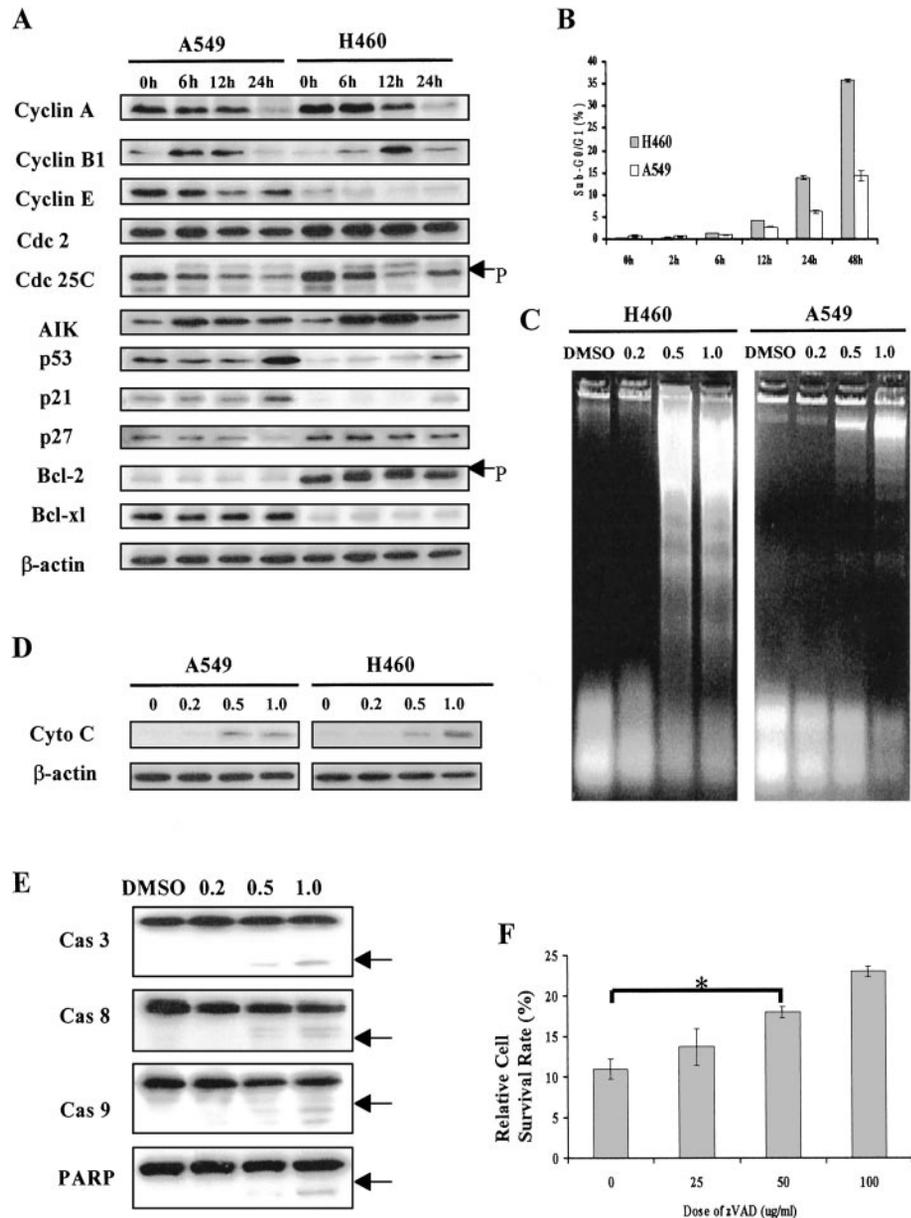
similar to those in cells treated with nocodazole (Fig. 3*F*) but completely different from the aggregated spindles present in paclitaxel-treated cells (Fig. 3*H*).

We then examined tubulin polymerization status in A549 cells after treatment with MZ, nocodazole, paclitaxel, or DMSO. At 4 h after treatment, tubulin polymerization status varied among the treatment conditions, but β-actin polymerization status did not (Fig. 3*I*). The ratio of depolymerized: polymerized tubulin was 0.75 ± 0.12 for MZ-treated A549 cells, 1.46 ± 0.25 for nocodazole-treated cells, 0.16 ± 0.03 for paclitaxel-treated cells, and 0.42 ± 0.06 for DMSO-treated control cells (Fig. 3*J*). Even 4 h of incubation with MZ was enough to enhance the depolymerization of tubulin in A549 cells, but the magnitude of this effect by MZ was significantly less than that by nocodazole.

In Vivo Tumor Suppression by MZ Treatment. We examined the therapeutic activity of MZ *in vivo* by giving oral doses to nude mice bearing s.c. tumors from H460 implants. To determine the effective dose of MZ *in vivo*, we performed dose-escalation experiments (data not shown). The preliminary results revealed that no side effects were observed in mice treated with 2 mg/mouse MZ every other day for 2 weeks and that a significant growth inhibition effect was confirmed in mice receiving a 1-mg dose of MZ. On the basis of these results, we treated mice bearing H460 tumor with 1 mg/mouse MZ. With a mean tumor volume of 14.8 mm³, mice were given MZ every other day for 3 weeks; water was used as a control. MZ significantly suppressed tumor growth by 14 days after the start of treatment (Fig. 4, *A* and *B*). TUNEL staining of 6-μm frozen sections of s.c. tumors in
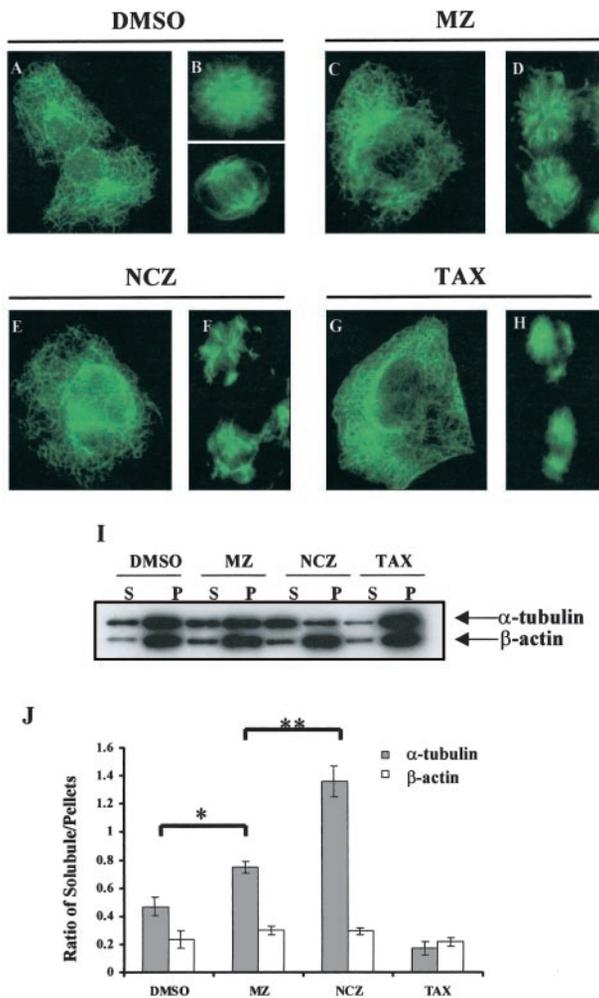
Fig. 3. MZ induces abnormal spindle formation and tubulin depolymerization in A549 cells. *A−H,* cells were grown on a glass chamber slide and treated with 0.1% DMSO (*A* and *B*), 0.5 μM MZ (*C* and *D*), 50 nM nocodazole (*NCZ*; *E* and *F*), or 10 nM paclitaxel (*TAX*; *G* and *H*) for 14 h. The cells were permeabilized, fixed, and stained with anti-α-tubulin antibody. *A, C, E,* and *G* represent the tubulin network in nonmitotic (interphase) cells. *B, D, F,* and *H* show representative spindle formations in mitotic cells. *I* and *J*, cells were treated with MZ, paclitaxel (*TAX*), or nocodazole (*NCZ*) for 4 h and then lysed and fractionated from cytosolic (soluble; *S*) to cytoskeletal (pellets; *P*) extracts. The extracts were separated with SDS-PAGE, transferred, and probed with both anti-α-tubulin and anti-β-actin antibodies. A representative immunoblot analysis in A549 cells is shown. *I,* intensity of each band of the immunoblot was measured by the NIH Image program, and the ratios of cytosolic and cytoskeletal tubulin and actin in each treatment were calculated in *J*. Values are mean ratios $\pm$ SD from three independent experiments. The significance level was set at $P < 0.05$. ∗, $P < 0.05$; ∗∗, $P < 0.01$.

untreated control animals and in MZ-treated mice revealed a significant fraction of apoptotic cells in MZ-treated tumors (Figs. 4*C*). These results suggest that MZ inhibits tumor cell growth *in vivo* by inducing apoptosis of tumor cells.

Next, we compared the efficacy of MZ with that of paclitaxel in experimental lung metastasis. The dose of paclitaxel *in vivo* was determined from the published data that used A549 cells in a pleural dissemination model (23). Results of the *in vivo* antitumor activity evaluation are summarized in Table 1. Single-drug therapy with MZ or paclitaxel did not

reduce body weight (data not shown). Paclitaxel treatment (i. p.) for 3 days alone did not reduce the number of lung colonies. However, oral administration of MZ (1 mg/mouse, every other day) showed antitumor activity as compared with controls, resulting in a 5-fold reduction in the number of lung colonies as compared with control untreated mice, without any toxicity to the mice.

Discussion

In this study, we found that MZ induced depolymerization of tubulin and inhibited normal spindle formation in NSCLC cells, resulting in mitotic arrest and cell death. This is the first direct evidence that MZ actively inhibits microtubule assembly in human NSCLC cells. Most microtubule-damaging agents that inhibit normal spindle formation, either by increasing microtubule stability or by depolymerization, can cause cells to arrest at the prometaphase/metaphase-to-anaphase transition (the mitotic checkpoint; Ref. 24). Our cell cycle and immunoblot analyses showed that MZ treatment also induced changes in the expression of cell cycle-regulatory proteins and initiated a phosphorylation cascade resulting in the phosphorylation of MPM-2 and Cdc25C in NCSLC cells. These dynamic changes in protein expression and modification are consistent with mitotic arrest (25).

MZ also induced apoptosis in NSCLC cells after mitotic arrest. The mechanism by which apoptosis is induced by microtubule-damaging agents is not completely understood. Even paclitaxel, which has been the most thoroughly investigated, seems to act on more than one pathway (26, 27). The complexity seems to be caused by differences in the cell types or drug concentration analyzed. However, the cytotoxicity of paclitaxel is thought to involve signaling that is different than that for DNA-damaging agents but is common to all microtubule-damaging agents, *i.e.,* mitotic arrest and the phosphorylation of specific proteins such as Bcl-2 or Bcl-xl (28). Several studies have already reported that phosphorylated Bcl-2/Bcl-xl does not homodimerize with Bax, resulting in increased levels of free Bax, a situation that may favor apoptosis (7, 22, 29). However, others contend that Bcl-2 phosphorylation takes place at G_2-M in normal cell cycle progression and is not associated with apoptosis after paclitaxel treatment (30–32). We observed Bcl-2 phosphorylation in H460 cells by 6–12 h after treatment with MZ but not in Bcl-2/Bcl-xl proteins in A549 cells, despite the fact that both cell lines showed apoptotic cells 24 h after MZ treatment. The time course of the change in the phosphorylation status of Bcl-2 in H460 cells seemed to be linked with that of MPM-2 and Cdc25C. These observations indicate that the phosphorylation of Bcl-2/Bcl-xl is neither common nor necessary for MZ-induced apoptosis in these NSCLC cell lines, but it may be associated with mitotic arrest.

In A549 and H460 cells, which have the wild-type p53 genotype, MZ induced p53 and p21 protein expression at 24 h of treatment. This up-regulation of p53 protein by MZ may have been caused by protein stabilization like that by paclitaxel (33). The induction of p53 and p21 may be involved in MZ-induced apoptosis, but the results of our cytotoxicity assay suggested that p53 status was not correlated with sensitivity of the cells to MZ. It has been reported that pa-
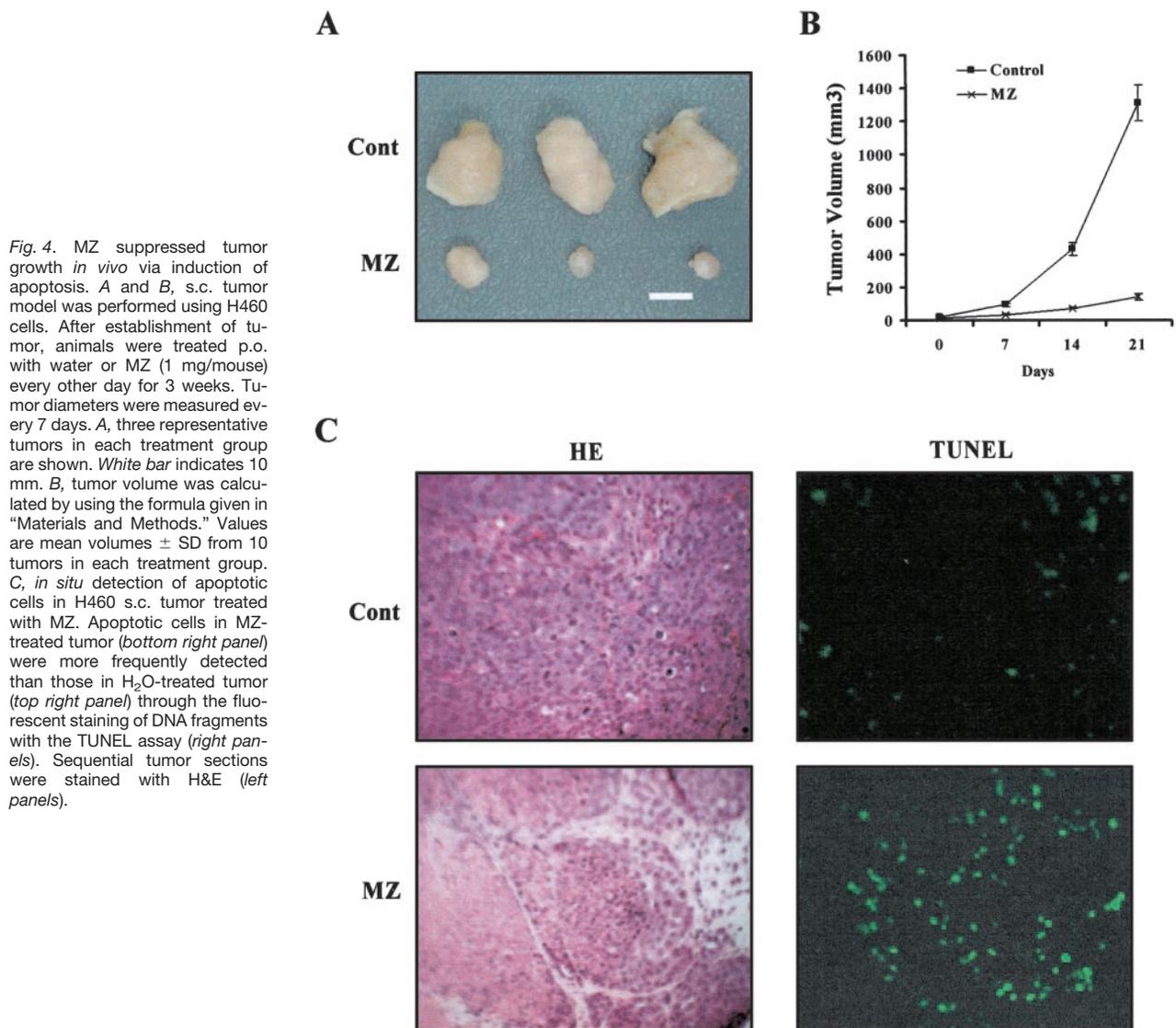
A

B

C

Fig. 4. MZ suppressed tumor growth *in vivo* via induction of apoptosis. *A* and *B,* s.c. tumor model was performed using H460 cells. After establishment of tumor, animals were treated p.o. with water or MZ (1 mg/mouse) every other day for 3 weeks. Tumor diameters were measured every 7 days. *A,* three representative tumors in each treatment group are shown. *White bar* indicates 10 mm. *B,* tumor volume was calculated by using the formula given in "Materials and Methods." Values are mean volumes $\pm$ SD from 10 tumors in each treatment group. *C, in situ* detection of apoptotic cells in H460 s.c. tumor treated with MZ. Apoptotic cells in MZ-treated tumor (*bottom right panel*) were more frequently detected than those in H$_2$O-treated tumor (*top right panel*) through the fluorescent staining of DNA fragments with the TUNEL assay (*right panels*). Sequential tumor sections were stained with H&E (*left panels*).

Table 1   Results of *in vivo* antitumor activity: numbers of lung colonies in nude mice after injection with human lung cancer cell line A549 cells

Experiments	Control untreated	Paclitaxel (1 mg/mouse)	Mebendazole (1 mg/mouse)
1	300	210	80
2	300	Dead	0
3	265	185	68
4	220	156	0
5	280	236	90

clitaxel-induced apoptosis is p53 independent (7, 34), but p53 status may influence cell cycle progression after mitotic arrest (24). Verdoodt *et al.* (35) and Tsuiki *et al.* (36) reported that functional p53 and its activation of the G$_1$ checkpoint might prevent the formation of hyperploid cells after mitotic arrest resulting from nocodazole treatment. These observations were consistent with our preliminary findings that even long-term (72–96 h) incubation with MZ rarely induced hy-

perploidy in H460 cells and that we could not establish resistance to MZ in H460 or A549 cells.

We showed that cytochrome *c* release and caspase activation were both involved in MZ-induced apoptosis. Although the dominant cascades from a cellular stress to apoptosis depend on the type of stress or cell used, many anticancer drugs induce apoptosis via mitochondrial and caspase 9-dependent pathways, especially in leukemia cells. Ferreira *et al.* (37, 38) reported that anticancer drugs induced apoptosis mostly by activating caspase 8, without Fas/Fas ligand signaling, in NSCLC cells, including H460. We clarified here that caspases 3, 8, and 9 were activated by MZ in H460 cells. Although further investigations are needed to quantify or compare activities of the various caspases after MZ treatment, caspase activation cannot be the only pathway by which MZ induces cell death, given our findings that z-VAD-FMK reversed growth inhibition by no more than 15% in H460 cells, even though the proportion of dead cells was more than 35%. These results suggest that MZ can induce

cell death via multiple pathways involving mitochondrial and caspase-dependent cascades.

MZ showed antitumor effects *in vivo*. As shown in TUNEL staining, one of the reasons for the antitumor effect *in vivo* by MZ may be induction of apoptosis. Recently, we reported that MZ inhibited tumor angiogenesis in mice using CD31 staining and an assay for hemoglobin (39). These findings indicated that significant reduction of tumor vasculature was another possible reason for the *in vivo* antitumor effect of MZ.

MZ showed little inhibition of normal fibroblast growth *in vitro*, and it induced suppression of H460 tumors with no side effects *in vivo*. In light of the clinical experience with long-term MZ treatment for alveolar echinococcosis (12, 13), we predict that the toxicity of MZ will be tolerable for cancer therapy. Morris *et al.* (15) recently reported a high incidence of neutropenia in a pilot study of albendazole for advanced cancer. However, because the hepatic metabolism of MZ differs from that of albendazole, the side effects in that study may not be applicable to therapy with MZ.

In summary, our results indicate that MZ, a well-known antiparasitic drug, may be useful as a microtubule inhibitor for lung cancer chemotherapy. However, our results also suggest that as compared with nocodazole, a well-known spindle inhibitor, MZ has less effect on mitotic spindle formation and in the depolymerization of tubulin in tumor cells. It has already been reported that some microtubule inhibitors possess pleiotropic effects that are independent of microtubule (40). Taken together, we speculate that tubulin depolymerization by MZ is perhaps not the only reason for the cell death. Studies of the schedule of administration and side effects of MZ in the treatment of cancer or investigations of the use of MZ in combination with other chemotherapeutic agents will further elucidate the potential usefulness of MZ as an anticancer drug.

Acknowledgments

References

1. Jemal, A., Thomas, A., Murray, T., and Thun, M. Cancer statistics, 2002. CA Cancer J. Clin., *52:* 23–47, 2002.

2. Bunn, P. A., Jr., Vokes, E. E., Langer, C. J., and Schiller, J. H. An update on North American randomized studies in non-small cell lung cancer. Semin. Oncol., *25:* 2–10, 1998.

3. Jordan, M. A., and Wilson, L. Microtubules and actin filaments: dynamic targets for cancer chemotherapy. Curr. Opin. Cell Biol., *10:* 123–130, 1998.

4. Sorenson, S., Glimelius, B., and Nygren, P. A systematic overview of chemotherapy effects in non-small cell lung cancer. Acta Oncol., *40:* 327–339, 2001.

5. Fossella, F. V., Lee, J. S., Murphy, W. K., Lippman, S. M., Calayag, M., Pang, A., Chasen, M., Shin, D. M., Glisson, B., and Benner, S. Phase II study of docetaxel for recurrent or metastatic non-small-cell lung cancer. J. Clin. Oncol., *12:* 1238–1244, 1994.

6. Kelly, K., Crowley, J., Bunn, P. A., Presant, C. A., Grevstadr, P. K., Moinpour, C. M., Ramsey, S. D., Wozniak, A. J., Weiss, G. R., Moore, D. F., Israel, V. K., Livingston, R. B., and Gandara, D. R. Randomized

7. Blagosklonny, M. V., Giannakakou, P., el-Deiry, W. S., Kingston, D. G., Higgs, P. I., Neckers, L., and Fojo, T. Raf-1/bcl-2 phosphorylation: a step from microtubule damage to cell death. Cancer Res., *57:* 130–135, 1997.

8. Laclette, J. P., Guerra, G., and Zetina, C. Inhibition of tubulin polymerization by mebendazole. Biochem. Biophys. Res. Commun., *92:* 417–423, 1980.

9. Gull, K., Dawson, P. J., Davis, C., and Byard, E. H. Microtubules as target organelles for benzimidazole anthelmintic chemotherapy. Biochem. Soc. Trans., *15:* 59–60, 1987.

10. Lacey, E., and Watson, T. R. Structure-activity relationships of benzimidazole carbamates as inhibitors of mammalian tubulin, *in vitro*. Biochem. Pharmacol., *34:* 1073–1077, 1985.

11. Eckert, J., Conraths, F. J., and Tackmann, K. Echinococcosis: an emerging or re-emerging zoonosis? Int. J. Parasitol., *30:* 1283–1294, 2000.

12. Muller, E., Akovbiantz, A., Ammann, R. W., Bircher, J., Eckert, J., Wissler, K., Witassek, F., and Wuthrich, B. Treatment of human echinococcosis with mebendazole. Preliminary observations in 28 patients. Hepatogastroenterology, *29:* 236–239, 1982.

13. Ammann, R. W., Ilitsch, N., Marincek, B., and Freiburghaus, A. U. Effect of chemotherapy on the larval mass and the long-term course of alveolar echinococcosis. Swiss Echinococcosis Study Group. Hepatology, *19:* 735–742, 1994.

14. Pourgholami, M. H., Woon, L., Almajd, R., Akhter, J., Bowery, P., and Morris, D. L. *In vitro* and *in vivo* suppression of growth of hepatocellular carcinoma cells by albendazole. Cancer Lett., *165:* 43–49, 2001.

15. Morris, D. L., Jourdan, J. L., and Pourgholami, M. H. Pilot study of albendazole in patients with advanced malignancy. Effect on serum tumor markers/high incidence of neutropenia. Oncology (Basel), *61:* 42–46, 2001.

16. Wyllie, A. H. Glucocorticoid-induced thymocyte apoptosis is associated with endogenous endonuclease activation. Nature (Lond.), *284:* 555–556, 1980.

17. Sudo, T., Ota, Y., Kotani, S., Nakao, M., Takami, Y., Takeda, S., and Saya, H. Activation of Cdh1-dependent APC is required for G_1 cell cycle arrest and DNA damage-induced G_2 checkpoint in vertebrate cells. EMBO J., *20:* 6499–6508, 2001.

18. Nakamura, S., Roth, J. A., and Mukhopadhyay, T. Multiple lysine mutation in the C-terminal domain of p53 interfere with mdm2-dependent protein degradation and ubiquitination. Mol. Cell. Biol., *20:* 9391–9398, 2000.

19. Hirota, T., Morisaki, T., Nishiyama, Y., Marumoto, T., Tada, K., Hara, T., Masuko, N., Inagaki, M., Hatakeyama, K., and Saya, H. Zyxin, a regulator of actin filament assembly, targets the mitotic apparatus by interacting with h-warts/LATS1 tumor suppressor. J. Cell Biol., *149:* 1073–1086, 2000.

20. Minotti, A. M., Barlow, S. B., and Cabral, F. Resistance to antimitotic drugs in Chinese hamster ovary cells correlates with changes in the level of polymerized tubulin. J. Biol. Chem., *266:* 3987–3994, 1991.

21. Ho, Y. S., Duh, J. S., Jeng, J. H., Wang, Y. J., Liang, Y. C., Lin, C. H., Tseng, C. J., Yu, C. F., Chen, R. J., and Lin, J. K. Griseofulvin potentiates antitumorigenesis effects of nocodazole through induction of apoptosis and G_2-M cell cycle arrest in human colorectal cancer cells. Int. J. Cancer., *91:* 393–401, 2001.

22. Poruchynsky, M. S., Wang, E. E., Rudin, C. M., Blagosklonny, M. V., and Fojo, T. Bcl-xL is phosphorylated in malignant cells following microtubule disruption. Cancer Res., *58:* 3331–3338, 1998.

23. Kraus-Berthier, L., Jan, M., Guilbaud, N., Naze, M., Pierré, A., and Atassi, G. Histology and sensitivity to anticancer drugs of two human non-small cell lung carcinomas implanted in the pleural cavity of nude mice. Clin. Cancer Res., *6:* 297–304, 2000.

24. Sorger, P. K., Dobles, M., Tournebize, R., and Hyman, A. A. Coupling cell division and cell death to microtubule dynamics. Curr. Opin. Cell Biol., *9:* 807–814, 1997.

Phase III trial of paclitaxel plus carboplatin *versus* vinorelbine plus cisplatin in the treatment of patients with advanced non-small cell lung cancer: a Southwest Oncology Group trial. J. Clin. Oncol., *19:* 3210–3218, 2001.

25. Morris, M. C., Heitz, A., Mery, J., Heitz, F., and Divita, G. An essential phosphorylation-site domain of human cdc25C interacts with both 14-3-3 and cyclins. J. Biol. Chem., *275:* 28849–28857, 2000.

26. Blagosklonny, M. V., and Fojo, T. Molecular effects of paclitaxel: myths and reality (a critical review). Int. J. Cancer, *83:* 151–156, 1999.

27. Wang, T. H., Wang, H. S., and Soong, Y. K. Paclitaxel-induced cell death: where the cell cycle and apoptosis come together. Cancer (Phila.), *88:* 2619–2628, 2000.

28. Wang, L. G., Liu, X. M., Kreis, W., and Budman, D. R. The effect of antimicrotubule agents on signal transduction pathways of apoptosis: a review. Cancer Chemother. Pharmacol., *44:* 355–361, 1999.

29. Haldar, S., Chintapalli, J., and Croce, C. M. Taxol induces bcl-2 phosphorylation and death of prostate cancer cells. Cancer Res., *56:* 1253–1255, 1996.

30. Ling, Y. H., Tornos, C., and Perez-Soler, R. Phosphorylation of Bcl-2 is a marker of M phase events and not a determinant of apoptosis. J. Biol. Chem., *273:* 18984–18991, 1998.

31. Scatena, C. D., Stewart, Z. A., Mays, D., Tang, L. J., Keefer, C. J., Leach, S. D., and Pietenpol, J. A. Mitotic phosphorylation of Bcl-2 during normal cell cycle progression and Taxol-induced growth arrest. J. Biol. Chem., *273:* 30777–30784, 1998.

32. Fan, M., Du, L., Stone, A. A., Gilbert, K. M., and Chambers, T. C. Modulation of mitogen-activated protein kinases and phosphorylation of Bcl-2 by vinblastine represent persistent forms of normal fluctuations at G_2-M_1. Cancer Res., *60:* 6403–6407, 2000.

33. Blagosklonny, M. V., Schulte, T. W., Nguyen, P., Mimnaugh, E. G., Trepel, J., and Neckers, L. Taxol induction of p21WAF1 and p53 requires c-raf-1. Cancer Res., *55:* 4623–4626, 1995.

34. Haldar, S., Basu, A., and Croce, C. M. Bcl2 is the guardian of microtubule integrity. Cancer Res., *57:* 229–233, 1997.

35. Verdoodt, B., Decordier, I., Geleyns, K., Cunha, M., Cundari, E., and Kirsch-Volders, M. Induction of polyploidy and apoptosis after exposure to high concentrations of the spindle poison nocodazole. Mutagenesis, *14:* 513–520, 1999.

36. Tsuiki, H., Nitta, M., Tada, M., Inagaki, M., Ushio, Y., and Saya, H. Mechanism of hyperploid cell formation induced by microtubule inhibiting drug in glioma cell lines. Oncogene, *20:* 420–429, 2001.

37. Ferreira, C. G., Tolis, C., Span, S. W., Peters, G. J., van Lopik, T., Kummer, A. J., Pinedo, H. M., and Giaccone, G. Drug-induced apoptosis in lung cnacer cells is not mediated by the Fas/FasL (CD95/APO1) signaling pathway. Clin. Cancer Res., *6:* 203–212, 2000.

38. Ferreira, C. G., Span, S. W., Peters, G. J., Kruyt, F. A., and Giaccone, G. Chemotherapy triggers apoptosis in a caspase-8-dependent and mitochondria-controlled manner in the non-small cell lung cancer cell line NCI-H460. Cancer Res., *60:* 7133–7141, 2000.

39. Mukhopadhyay, T., Sasaki, J., Ramesh, R., and Roth, J. A. Mebendazole elicits a potent antitumor effect on human cancer cell lines both *in vitro* and *in vivo*. Clin. Cancer Res., *8:* 2963–2969, 2002.

40. Molero, J. C., Whitehead, J. P., Meerloo, T., and James, D. E. Nocodazole inhibits insulin-stimulated glucose transport in 3T3–L1 adipocytes via a microtubule-independent mechanism. J. Biol. Chem., *276:* 43829–43835, 2001.

The Anthelmintic Drug Mebendazole Induces Mitotic Arrest and Apoptosis by Depolymerizing Tubulin in Non-Small Cell Lung Cancer Cells 1 Supported in part by grants from the National Cancer Institute and the NIH Specialized Program of Research Excellence in Lung Cancer P-50-CA70907 and P01 CA78778-01A1 (both to J. A. R.), by gifts to the Division of Surgery and Anesthesiology from Tenneco and Exxon for the Core Laboratory Facility, by The University of Texas M. D. Anderson Cancer Center Support Core Grant CA16672, by the W. M. Keck Foundation, and by a sponsored research agreement with Introgen Therapeutics, Inc. J. A. R. is a scientific advisor for Introgen Therapeutics, Inc. 1

Ji-ichiro Sasaki, Rajagopal Ramesh, Sunil Chada, et al.

Updated version	Access the most recent version of this article at: http://mct.aacrjournals.org/content/1/13/1201

Cited articles	This article cites 40 articles, 21 of which you can access for free at: http://mct.aacrjournals.org/content/1/13/1201.full#ref-list-1
Citing articles	This article has been cited by 7 HighWire-hosted articles. Access the articles at: http://mct.aacrjournals.org/content/1/13/1201.full#related-urls

E-mail alerts	Sign up to receive free email-alerts related to this article or journal.
Reprints and Subscriptions	To order reprints of this article or to subscribe to the journal, contact the AACR Publications Department at pubs@aacr.org.
Permissions	To request permission to re-use all or part of this article, use this link http://mct.aacrjournals.org/content/1/13/1201. Click on "Request Permissions" which will take you to the Copyright Clearance Center's (CCC) Rightslink site.